BJR

https://doi.org/10.1259/bjr.20190004

Received: 22 December 2018 | Revised: 09 May 2019 | Accepted: 15 May 2019

Cite this article as:
Ueda Y, Ohira S, Yamazaki H, Mabuchi N, Higashinaka N, Miyazaki M, et al. Dosimetric performance of two linear accelerator-based radiosurgery systems to treat single and multiplebrain metastases. *Br J Radiol* 2019; **92**: 20190004.

FULL PAPER

Dosimetric performance of two linear accelerator-based radiosurgery systems to treat single and multiplebrain metastases

[1]YOSHIHIRO UEDA, MS, [1]SHINGO OHIRA, PhD, [2]HIDEYA YAMAZAKI, MD, PhD, [2]NOBUHISA MABUCHI, MD, PhD, [2]NAOKAZU HIGASHINAKA, [1]MASAYOSHI MIYAZAKI, BS and [1]TERUKI TESHIMA, MD, PhD

[1]Department of Radiation Oncology, Osaka International Cancer Institute, Osaka, Japan
[2]Department of Radiation Oncology, Soseikai General Hospital CyberKnife Center, Kyoto, Japan

Address correspondence to: Mr Yoshihiro Ueda
E-mail: *ueda-yo@mc.pref.osaka.jp*

Objective: To evaluate and compare the dosimetric plan quality for noncoplanar volumetric arc therapy of single and multiple brain metastases using the linear accelerator-based radiosurgery system HyperArc and a robotic radiosurgery system.
Methods: 31 tumors from 24 patients were treated by stereotactic radiosurgery using the CyberKnife system. CT images, structure sets, and dose files were transferred to the Eclipse treatment planning system for the HyperArc system. Dosimetric parameters for both plans were compared. The beam-on time was calculated from the total monitor unit and dose rate.
Results: For normal brain tissue, the received volume doses were significantly lower for HyperArc than for CyberKnife_G4 and strongly correlated with the planning target volume (PTV) for cases of single brain metastasis. In addition, the difference in volume dose between CyberKnife_G4 and HyperArc was proportional to the PTV. For multiple brain metastases, no significant difference was observed between the two stereotactic radiosurgery systems, except for high-dose region in the normal tissue. In low dose for brain minus PTV, when the maximum distance among each target was above 8.0 cm, HyperArc delivered higher dose than CyberKnife_G4. The mean ± SDs for the beam-on time were 15.8 ± 5.3 and 5.6 ± 0.8 min for CyberKnife_G4 and HyperArc, respectively ($p < .01$).
Conclusion: HyperArc is best suited for larger targets in single brain metastasis and for smaller inter tumor tumor distances in multiple brain metastases.
Advances in knowledge: The performance of HyperArc in comparison with CyberKnife_G4 was depended on defined margin and tumor distances.

INTRODUCTION

Brain metastases occur in 20–40% of patients suffering systemic cancer,[1] and stereotactic radiosurgery (SRS) offers an effective clinical treatment. In fact, the aggressive treatment of brain metastases improves the prognosis of patients,[2] increasing their life expectancy. However, there is increased possibility that other brain metastases appear in different locations. For brain metastasis reirradiation, it is important to increase the normal brain sparing by accurately concentrating the dose to the tumor. For a highly concentrated tumor dose, several systems have been developed for clinical use,[3] including radiosurgery systems based on γ knife and linear accelerator, where the latter mainly comprises two methods: CyberKnife (Accuray, Inc., Sunnyvale, CA, USA) and volumetric modulated arc therapy (VMAT) with generic linear accelerators.

In CyberKnife, a linear accelerator is mounted on and controlled using a flexible robotic arm. To achieve a higher dose concentration, several hundred treatment beams from over a thousand possible beam directions are used. These beams are delivered in either an isocentric manner via circular collimators of varying sizes[4] or a non-isocentric manner using multiple pencil beams.[5]

For SRS, VMAT with flattening filter-free beams provides a high dose rate to the target and shortens the treatment time compared with the traditional flattening filter beams.[6–8] A novel VMAT system called HyperArc (Varian Medical Systems, Inc., Palo Alto, CA, USA) employed along with improved planning strategies aims to achieve higher conformity.[9–11] In fact, Ohira et al[9] and Slosarek et al[11] found that HyperArc delivers a lower dose to the brain compared with standard noncoplanar VMAT given its optimization algorithm for SRS–VMAT.

In this study, we compared the dosimetric plan quality of HyperArc and CyberKnife for a single target. The outcomes from this study can serve as guidelines to select the most suitable machine to treat single and multiple brain metastases.

METHODS AND MATERIALS

Patient data and CyberKnife treatment planning

45 tumors from 28 patients were treated using a CyberKnife model G4 (Accuray, Inc.) at the CyberKnife Center, Soseikai General Hospital, Kyoto, Japan. 31 of the tumors in 24 patients were treated for single targets and the remaining 14 tumors in 4 patients were treated for multiple targets. Written informed consent was obtained from all patients, and the Institutional Ethics Committee approved this study (Osaka International Cancer Institute review board number: 1706089007). Tables 1 and 2 list the tumor location, size and number per treatment and case.

A SCENARIA CT scanner was employed (Hitachi, Ltd., Tokyo, Japan). The CT images at slice thicknesses of 1.00 or 1.25 mm, 512 × 512 pixel matrix, and field of view of 35 cm were transferred to the Multiplan treatment planning system (Accuray, Inc.). For gross tumor volume delineation, a T_1 weighted MRI scan with contrast medium (gadolinium) was registered to the CT images.

Table 1. Information used in this study of patients treated with CyberKnife G4

Patient	Tumor	Sex	Tumor location	PTV [cm^3]	Marginal dose [%]	Number of beams
1	1	M	Right temporal lobe	0.97	94.16	37
2	2	F	Right parietal lobe	1.3	93.81	42
3	3	F	Right temporal lobe	4.4	79.17	102
4	4	F	Left cerebellum	0.03	86.94	34
5	5	F	Cerebellum	2.6	87.16	135
6	6	F	Right occipital lobe	0.2	90.37	41
6	7	F	Right temporal lobe	0.1	91.91	41
7	8	F	Right temporal lobe	1.1	93.94	42
8	9	F	Right temporal lobe	0.65	89.29	42
9	10	M	Left temporal lobe	0.1	86.51	42
10	11	M	Right occipital lobe	0.21	93.77	41
10	12	M	Right thalamus	0.1	82.09	41
10	13	M	Left parietal lobe	0.04	88.13	42
10	14	M	Right cerebellum	0.04	90.61	42
11	15	M	Right frontal lobe	0.01	98.65	30
11	16	M	Right temporal lobe	0.02	98.15	37
11	17	M	Right parietal lobe	0.02	97.55	40
11	18	M	Right temporal lobe	0.03	90.16	52
12	19	F	Left frontal lobe	0.01	97.83	42
13	20	M	Left occipital lobe	0.01	96.28	42
14	21	M	Right frontal lobe	0.7	90	35
15	22	F	Right occipital lobe	0.7	93.05	41
16	23	M	Right temporal lobe	0.2	79.39	30
17	24	M	Left parietal lobe	2.6	91.74	72
18	25	M	Right frontal lobe	0.1	90.24	25
19	26	M	Right parietal lobe	1.7	91.36	39
20	27	F	Right cerebellum	0.06	91.52	40
21	28	F	Left occipital lobe	0.1	89.09	38
22	29	F	Left parietal lobe	0.012	95.17	42
23	30	M	Left occipital lobe	0.9	81.4	24
24	31	F	Left temporal lobe	2.7	93.99	42

F, female; M, male; PTV, planning target volume.

Table 2. Information used in this study of patients treated with CyberKnife G4 for multiple brain metastasis cases

Patient	Plan	Tumor num.	Sex	Tumor locations	Total PTV [cm^3]	Marginal dose [%]	Number of beams
1	1	3	F	Right temporal lobe	0.54	91.25	118
2	2	3	F	Right parietal lobe, right basal ganglia, and left frontal lobe	0.17	94.29	42
3	3	3	F	Right cerebrum	1.7	87.45	125
3	4	3	F	Right temporal lobe	0.71	94.43	126
4	5	2	F	Right temporal lobe	0.03	90.16	52

F, female; M, male; PTV, planning target volume.

The planning target volume (PTV) was created by adding no margin to the gross tumor volume (GTV). The CyberKnife_G4 planning was performed by inverse planning. An optimization algorithm (Raytracing) using grid size of 1.25 mm was iterated until it achieved the institutional ideal dose distribution determined by physicians. The obtained number of beams are listed in Tables 1 and 2. The dose was prescribed to the isodose line conforming to the PTV. The marginal dose in each plan was defined as the percentage (100% represents the maximum dose) of an isodose curve covering the PTV and is also listed in Table 1. For normalization, a dose of 25 Gy in one fraction was used as prescribed dose.

For the dose–volume constraints in organs at risk (OARs), we used the development by Timmerman et al.[12] Specifically, the constraints followed that $D_{0.2}$ (*i.e.,* doses expressed in grays to 0.2 cm^3 of the volume) of the optic pathway reached up to 8 Gy, D_1 (*i.e.,* doses expressed in grays to 1 cm^3 of the volume) of the brainstem reached up to 10 Gy, and V_{14} (*i.e.,* volume receives doses exceeding 14 Gy) of whole brain minus PTV reached up to 7 cm^3. In cases with some plans, such as patients 6, 10, and 11 in Table 1, the accumulated dose from all plans was evaluated for dose constraining.

HyperArc treatment planning

The CT images and structure sets used for the CyberKnife_G4 treatment planning were transferred to a treatment planning system prototype (Eclipse v. 15.5, Varian Medical Systems, Inc., Palo Alto, CA, USA.). All HyperArc plans were designed on the Edge radiosurgery system with a high-resolution multileaf collimator, 2.5 mm leaf width (Varian Medical Systems, Inc., Palo Alto, CA, USA.). During HyperArc planning, various parameters are automatically optimized. For instance, the isocenter is positioned at the center of the PTV, and the collimator angle and field size are optimized to reduce the dose to OARs and normal tissues depending on the structures. In addition, four arc fields, three of which are noncoplanar, are also arranged: one full or half coplanar arc with couch rotation of 0° and three half noncoplanar arcs with couch rotations of 315, 45, and 90° (or 270°). Virtual dry run function was implemented to stave off collision of a gantry and a couch during four arcs.

The photon beam energy used for the arcs was 6 MV flattening filter-free. Inverse treatment planning for HyperArc was performed using Photon Optimizer (Varian Medical Systems, Inc., Palo Alto, CA, USA.) with optimization resolution of 1.25 mm. An SRS normal tissue objective (NTO) was used to generate treatment plans with steep dose decays in space from target-specific dose levels to low asymptotic dose levels. The objective automatically recognizes spatial arrangements of targets for which dose bridging among targets is likely to occur and attempts to prevent dose bridging at levels higher than 17% of the prescription. In the HyperArc treatment plan, optimization was repeated for the PTV dose, such as D_{95} and D_2 (*i.e.,* doses expressed in grays to 95 and 2% of the volume, respectively), matched with those of the CyberKnife_G4 treatment plan. To obtain the dose distribution, the lower and upper objectives were set at PTV. As lower objective, the average of D_{100} was 24.2 ± 0.7 Gy. As upper

Figure 1. Dose distributions for CK and HA with target volumes of 0.1 (A, B) and 4.4 cm^3 (C, D) in single metastasis cases. The colored lines represent different isodose lines. Cyan and white represent the low-isodose lines of 3.0 and 6.0 Gy, respectively. At target volume of 4.4 cm^3, the isodose volume for HA is clearly smaller than that for CK. CK,CyberKnife; HA, HyperArc; PTV, planning target volume.

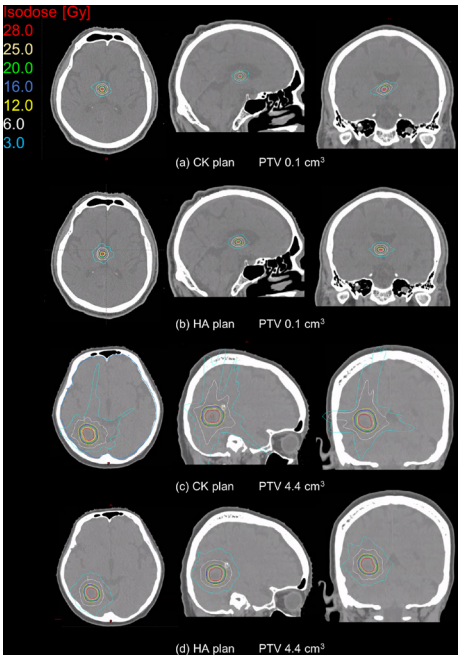

objective, the average of D_0 was 27.7 ± 1.6 Gy. In OARs, there was no upper objective for organs during optimization. For dose calculation, the anisotropic analytical algorithm was used with grid size of 1.25 mm.

Data analysis

To assess treatment plan quality, dosimetric parameters were calculated from the dose volume histogram of the PTV and normal tissues of the brain, brain stem, optic chiasma, optic nerves (ONs), and eyes. The homogeneity index (HI), conformity index (CI), and gradient index (GI) were defined as

$$\frac{Dmax}{Dprescribed},$$

$$\frac{TVPV^2}{(TV \times PV)},$$

$GI = \frac{PV50}{PV}$,where D*max* and D*prescribed* denote the maximum and prescribed doses, respectively,[13] CI is a measure of the radiation distribution fitness to the shape of the radiosurgical target, TVPV, TV, and PV represent the volume of the target covered by the prescription dose, target volume, and prescription isodose volume, respectively,[14] GI represents the dose fall-off, and PV50 denotes 50% of the prescription isodose volume.[14] In normal tissues except for the brain, D*mean* denotes the mean dose and D_{98} is the dose expressed in grays to 98% of the volume. To evaluate the sparing rate in the brain, its region minus PTV ratio that receives doses exceeding 21, 18, 15, 12, 6, and 3 Gy (V_{21}, V_{18}, V_{15}, V_{12}, V_6, and V_3, respectively) were determined. Finally, to determine the treatment efficacy, the beam-on time per tumor was calculated as

Beam-on time [min]=Total monitor unit/dose rate [μ/min].

The set dose rates were 800 μ/min and 1400 μ/min for CyberKnife_G4 and HyperArc, respectively. In every field for HyperArc plan, the dose rate was maintained at the maximum of 1400 μ/min.

Statistical analysis

The Wilcoxon signed-rank test implemented on the Statistical Package for the Social Sciences (IBM Co., New York, USA) was used to determine significant differences among the corresponding system indices in the two systems.

RESULTS

The dose distributions for small and large targets for single brain metastasis cases in the axial, sagittal and coronal planes are shown in Figure 1. The volume of the small target was 0.1 cm^3 and that of the large target was 4.4 cm^3. In the small target, the expansion of isodose lines was similar for both CyberKnife_G4 and HyperArc, whereas in the large target, low isodose lines such as 6.0 and 3.0 Gy for CyberKnife_G4 were clearly larger than those for HyperArc.

Table 3 summarizes some dosimetric parameters for the PTV and OAR in single metastasis cases. In the PTV, no significant differences were found for D_2, D_{95}, D_{98}, and HI. In contrast, significant differences were found for CI and GI. Figure 2(a) shows the relationships between PTV and GI values. Indeed, the GI values were highly dependent on the target volume in CyberKnife_G4 and HyperArc. The mean ± SD of the differences among GI for CyberKnife_G4 and HyperArc was 0.7 ± 9.5. Figure 2(b) shows the relationships between PTV and these differences. When the PTV is below 0.03, the GI differences for CyberKnife_G4 and HyperArc exhibit large variations.

In the volume of the brain minus PTV, V_3, V_6, V_{12}, V_{15}, V_{18}, and V_{21} *i.e.* volumes receiving more than 3, 6, 12, 15, 18, and 21 Gy, respectively, for HyperArc were significantly smaller than those for CyberKnife_G4, as shown in Table 3. The D*mean* values are equal for CyberKnife and HyperArc. Box plots of the dose for the brain minus PTV are shown in Figure 3. In V_3, V_6, and V_{12}, the maximum value, upper whisker, and upper quartiles for HyperArc were lower than those for CyberKnife_G4. The median value was almost the same for CyberKnife_G4 and HyperArc.

In Figure 4, the dose for the brain minus PTV plotted against PTV is depicted for each treatment system. For both systems, strong correlations above 0.88 were found between dose and PTV. Notably, the OAR sparing for HyperArc increased with the PTV. The estimated dose for brain minus PTV was described with linear regression for both systems. CyberKnife can track the patients' position during irradiation, and thus eliminates setup errors. On the other hand, HyperArc cannot track the patients' position during irradiation and may

Table 3. Dosimetric comparison between CyberKnife and HyperArc for single and multiple brain metastasis

		Single brain metastasis (31 plans)			Multiple brain metastasis (five plans)		
Structure	**Dosimetric parameters**	**CyberKnife**	**HyperArc**		**CyberKnife**	**HyperArc**	
		Mean ± SD	**Mean ± SD**	*p* value	**Mean ± SD**	**Mean ± SD**	*p* value
PTV	**D_2 [Gy]**	27.5 ± 1.5	27.5 ± 1.3	.55	27.3 ± 0.9	27.3 ± 0.7	.55
	D_{98} [Gy]	24.8 ± 0.3	24.9 ± 0.3	.33	25.0 ± 0.4	25.1 ± 0.4	.33
	D_{95} [Gy]	25.2 ± 0.2	25.2 ± 0.2	.91	25.3 ± 0.3	25.4 ± 0.3	.91
	HI	1.1 ± 0.1	1.1 ± 0.1	.55	1.1 ± 0.0	1.1 ± 0.0	.55
	GI	14.6 ± 19.5	14.1 ± 25.1	<.01	9.6 ± 5.0	13.9 ± 8.9	.08
	CI	0.6 ± 0.2	0.8 ± 0.2	<.01	0.4 ± 0.2	0.7 ± 0.2	<.01
Brain sub. PTV	**V_{21} [cm^3]**	1.3 ± 1.6	0.5 ± 0.5	<.01	2.1 ± 1.2	1.1 ± 0.7	<.05
	V_{18} [cm^3]	2.0 ± 2.4	0.9 ± 0.8	<.01	3.3 ± 1.8	2.0 ± 1.2	<.05
	V_{15} [cm^3]	2.9 ± 3.3	2.0 ± 2.3	<.01	4.7 ± 2.5	3.5 ± 2.0	<.05
	V_{12} [cm^3]	4.1 ± 4.7	2.1 ± 2.0	<.01	6.8 ± 3.5	5.8 ± 3.2	.13
	V_6 [cm^3]	11.9 ± 13.9	6.6 ± 6.3	<.01	21.9 ± 10.6	21.7 ± 11.3	.94
	V_3 [cm^3]	35.0 ± 43.6	18.7 ± 18.7	<.01	83.7 ± 47.1	93.9 ± 59.4	.38
Brain stem	**D_{mean} [Gy]**	0.4 ± 0.6	0.2 ± 0.3	.45	0.6 ± 0.4	1.0 ± 0.5	.07
	D_2 [Gy]	1.0 ± 1.4	0.7 ± 0.6	.05	1.1 ± 1.3	1.4 ± 1.1	.11
Optic chiasm	**D_{mean} [Gy]**	0.3 ± 0.5	0.2 ± 0.2	.29	0.7 ± 0.7	0.6 ± 0.6	.91
	D_2 [Gy]	0.7 ± 0.9	0.4 ± 0.4	.04	1.4 ± 1.0	1.3 ± 0.7	.80
Left ON	**D_{mean} [Gy]**	0.2 ± 0.6	0.2 ± 0.3	.61	0.4 ± 0.4	0.5 ± 0.4	.86
	D_2 [Gy]	0.6 ± 1.1	0.4 ± 0.5	.77	0.5 ± 0.7	0.6 ± 0.7	.76
Right ON	**D_{mean} [Gy]**	0.2 ± 0.3	0.2 ± 0.2	.72	0.6 ± 0.4	0.6 ± 0.4	.56
	D_2 [Gy]	0.6 ± 0.7	0.4 ± 0.3	.09	0.9 ± 0.9	0.9 ± 0.7	.70
Left eye	**D_{mean} [Gy]**	0.1 ± 0.1	0.1 ± 0.1	.32	0.1 ± 0.2	0.2 ± 0.1	.83
	D_2 [Gy]	0.2 ± 0.3	0.1 ± 0.1	.36	0.4 ± 0.4	0.2 ± 0.1	.34
Right eye	**D_{mean} [Gy]**	0.1 ± 0.2	0.1 ± 0.1	.02	0.5 ± 0.6	0.2 ± 0.1	.27
	D_2 [Gy]	0.2 ± 0.3	0.2 ± 0.1	.23	0.7 ± 0.7	0.3 ± 0.1	.23

D*x*, dose *x*% of volume; CI, conformity index; GI, gradient index; HI, homogeneity index; ON, optic nerve; PTV, planning target volume; SD, standard deviation; V*x*, the organ-at-risk volume ratio that receives a dose exceeding *x* Gy.

require some margin for PTV. Figure 4 shows the estimated dose obtained from as triangles in gray and yellow adding to 1- and 2 mm margins. Adding margin to the PTV, V_3 and V_6 for HyperArc is almost the same as that for CyberKnife_G4. V_{12} for HyperArc is larger than that for CK. Figure 5 shows the changing dose distributions for HyperArc at GTV-to-PTV margin of 0, 1, and 2 mm in the same cases of Figure 1. The expansion of the isodose line is clear when margin increases. For the small target (Figure 5 (a)), the irradiated volumes V_3 and V_{12} adding 1 mm to the margin were 2.1 and 2.6 times as large as the no-margin PTV, and adding 2 mm 2.8 and 3.5 times, respectively. For the large target (Figure 5 (b)), the irradiated volumes V_3 and V_{12} adding a 1 mm margin were both 1.6 times as large as the no-margin PTV, and adding 2 mm 1.9 and 1.8 times, respectively.

The dose distributions for cases of multiple brain metastases in the axial, sagittal, and coronal planes are shown in Figure 6. These cases exhibit different distances among targets. For short distance among targets (Figure 6 (a) and (b)), the expansion of isodose lines was similar for both CyberKnife_G4 and HyperArc, whereas for larger distances (Figure 6 (c) and (d)), low isodose lines such as those at 3.0 Gy for HyperArc were clearly larger than those for CyberKnife_G4. In Figure 6 (a) and (b), V_6 and V_3 for brain minus PTV in CyberKnife_G4 were 28.2 and 91.4 cm^3 and in HyperArc were 21.0 and 78.1 cm^3, respectively. In Figure 6 (c) and (d), V_6 and V_3 for brain minus PTV in CyberKnife_G4 were 27.5 and 110.1 cm^3 and in HyperArc were 30.8 and 142.7 cm^3, respectively.

Table 3 also summarizes some dosimetric parameters for the PTV and OARs in cases of multiple metastases. There are significant differences for CI, V_{15}, V_{18}, and V_{21}. In V_{12}, V_6 and V_3 for brain minus PTV, there was no significant difference between CyberKnife_G4 and HyperArc. In three of the five plans, V_6 and V_3 for HyperArc were larger than those for CyberKnife.

Figure 2. (a) PTV according to GI. Blue represents CyberKnife, and orange represents HyperArc. GI is expressed in logarithmic scale. The GI for CyberKnife and HyperArc suitably fitting with the PTV. The dashed lines represent regression curves. (b) The relationships between PTV and the differences. The volume of the PTV is expressed in logarithmic scale. The red dotted line represents X coordinate of 0.03. GI, gradient index; PTV, planning target volume.

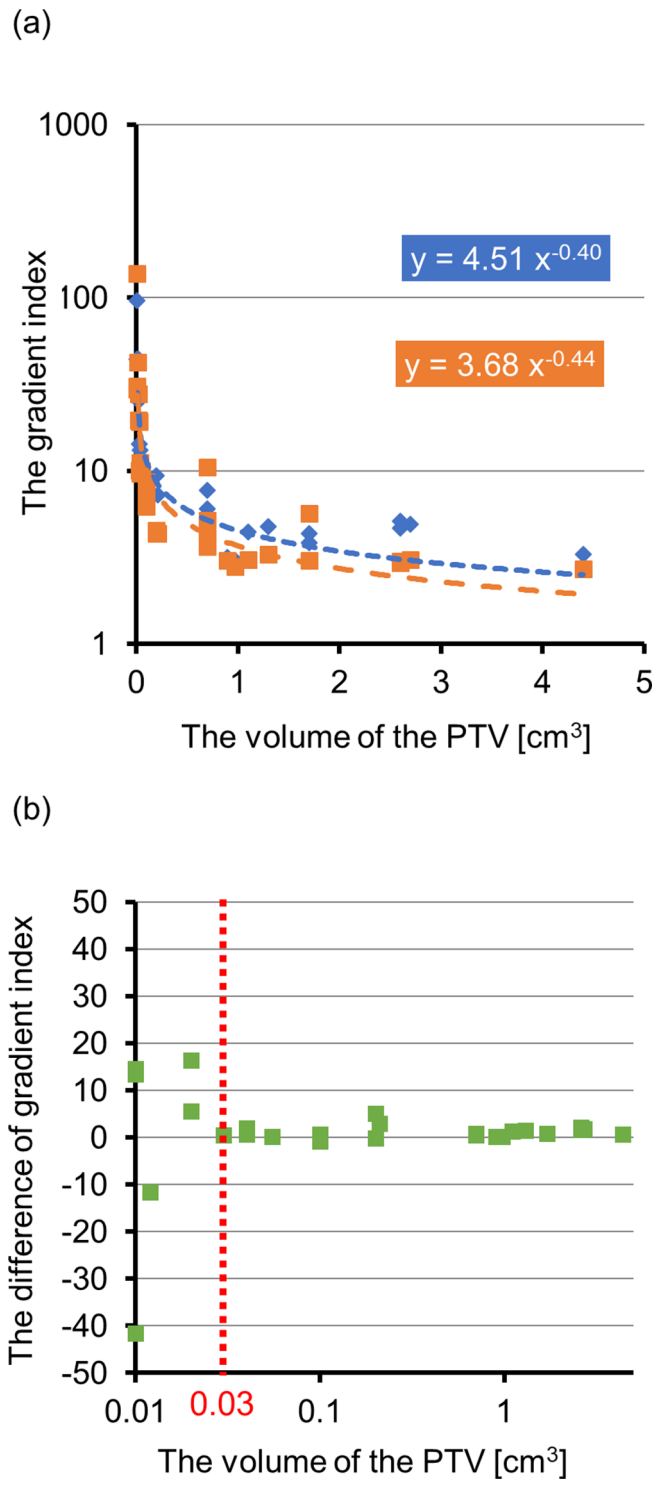

Figure 3. Box plots of (A) V_3, (B) V_6, and (C) V_{12} for brain minus PTV in CyberKnife (CK) and HyperArc (HA). CK is represented in blue, and HA is represented in orange. CK, CyberKnife; HA, HyperArc; PTV, planning target volume.

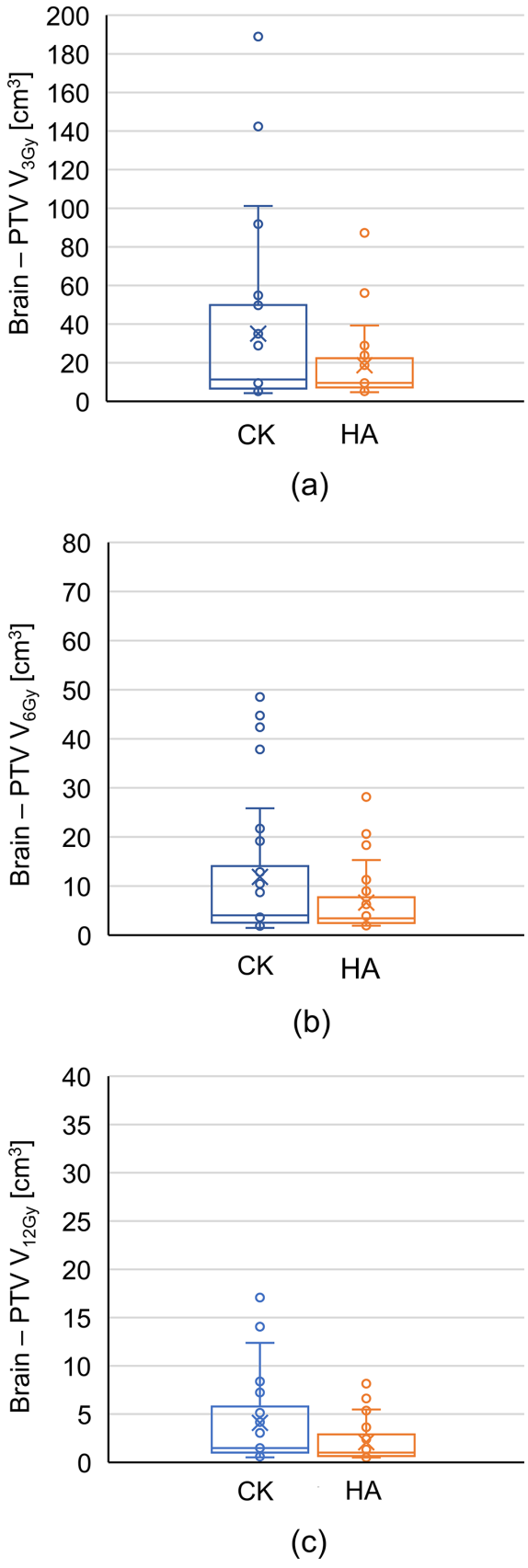

Figure 4. Relations between PTV and brain doses at (A) V_3, (B) V_6, and (C) V_{12}. CK is represented in blue, and HA is represented in orange. The relations are fitter using linear regression with coefficient of determination R^2. The regression dotted line slopes for HA are lower than those for CK in each case. As the difference in dose becomes larger, the PTV increases. Triangles represents the estimated dose with regression for HA when 1 (gray) and 2 mm (yellow) margins in every direction are added to the PTV. For V_3 and V_6, the 2 mm margin added to the PTV matches the regression line for the estimated dose in HA and CK, whereas in V_{12}, the matching occurs for the 1 mm margin. CK, CyberKnife; HA, HyperArc; PTV, planning target volume.

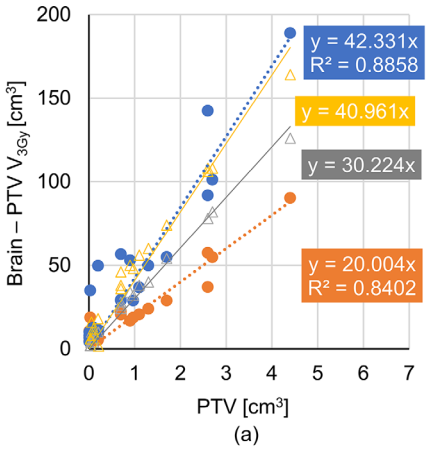

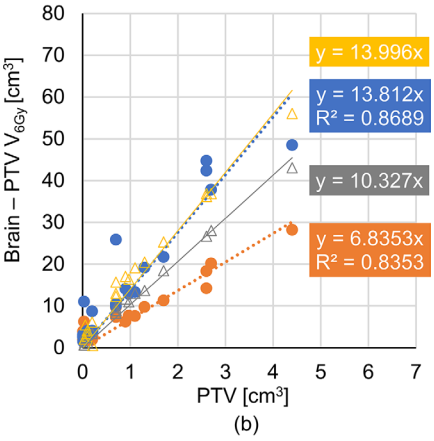

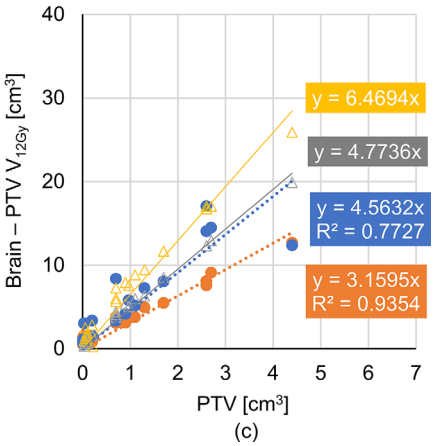

Figure 5. Dose distribution for HyperArc at GTV-to-PTV margin increments of 1 mm for (A) small and (B) large targets. Each colored line represents an isodose line, where cyan and white represent low-isodose lines at 3.0 and 6.0 Gy, respectively. GTV, gross tumor volume; PTV, planning target volume.

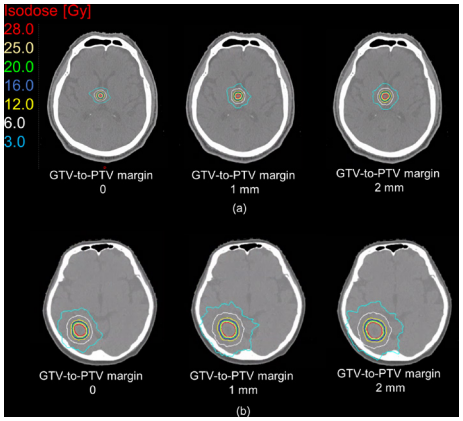

The mean differences ± SD for V_6 and V_3 between HyperArc and CyberKnife were 3.7 ± 2.3 and 26.9 ± 6.0 cm^3. These cases exhibited the maximum distances among tumor centers, being above 8.0 cm. Other two cases exhibited maximum distances below 5.0 cm.

The mean ± SD for beam-on time was 15.8 ± 5.3 and 5.6 ± 0.8 min for CyberKnife_G4 and HyperArc, respectively ($p < .01$).

Figure 6. Dose distributions for CK and HA with target volumes of (A, B) 0.5 and (C, D) 0.7 cm^3 in cases of multiple metastases. The maximum distance between each tumor were (A, B) 4.7 and (C, D) 9.2 cm. Each colored line represents an isodose line, where cyan and white represent low-isodose lines at 3.0 and 6.0 Gy, respectively. CK, CyberKnife; HA, HyperArc; PTV, planning target volume.

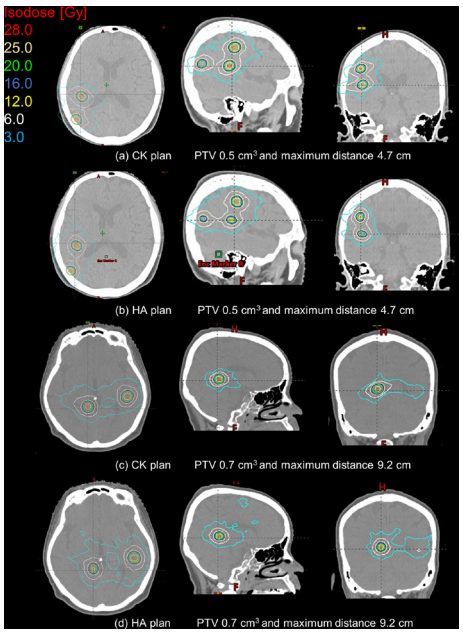

The correlation values between beam-on time and PTV were 0.58 and –0.27 for CyberKnife_G4 and HyperArc, respectively.

DISCUSSION

We analyzed the dose distributions for CyberKnife_G4 and HyperArc to single and multiple targets in this study, whereas previously, Ruggieri et al[10] analyzed multiple targets of brain metastases, and HyperArc significantly outperformed CyberKnife_G4. Still, as reirradiation is one strategy for recurring brain metastases,[15–18] plans with more conformity should be determined even for a single target.

In this study, the dose for the PTV in the HyperArc treatment plan was almost equal to that in the CyberKnife_G4 treatment plan, but the center dose can be increased when using HyperArc, consequently increasing OAR sparing. However, to guarantee a fair comparison between CyberKnife_G4 and HyperArc, we created every plan for both systems with the same PTV dose. In the CyberKnife system, the patients' positions during treatment are monitored using fluoroscopy, and intrafraction motions are dynamically compensated.[19–22] Therefore, the clinical target volume to PTV margin is extremely small in CyberKnife. On the other hand, no data were available on intrafraction motion for HyperArc. Consequently, it remains to be evaluated whether the margin for CyberKnife is acceptable for HyperArc, although the latter detects the patient's position between arcs using an onboard imaging system. OAR sparing is shown in Figure 4 adding setup margin for HyperArc. OAR sparing for HyperArc is less than or equal to CyberKnife. These results indicated the importance of the patient immobilization in HyperArc.

In multiple cases, unlike the study by Slosarek et al,[11] we found no significant difference between CyberKnife_G4 and HyperArc in dose volumes V_3, V_6, and V_{12} for the brain minus PTV. Specifically, in cases where the maximum distance among tumors is above 8.0 cm, HyperArc did not reduce the brain dose compared to CyberKnife_G4. This generally occurs in VMAT using generic linear accelerators because multileaf collimators cannot completely shield radiation to normal tissue between tumors. This problem was mitigated in HyperArc planning[11] and does not occur in CyberKnife planning. Therefore, in multiple distant tumors, HyperArc cannot reduce the low dose compared to CyberKnife_G4.

The CI and GI for HyperArc were better than those for CyberKnife_G4, as in the treatment plan for the latter, conformity only improves with more beams. However, there is a tradeoff between the number of beams and treatment time. We found a mean beam-on time for the CyberKnife_G4 treatment plan above 10 min. Hence, it is difficult to increase number of beams for this kind of treatment as CyberKnife uses a large number of static beams. Now, CyberKnife equipped with multileaf collimators, CyberKnife_M6, has been developed and used in clinical practice. If CyberKnife is developed to use arc beam, the CI and GI may be better than those for HyperArc. Because CyberKnife is able to select various arc beams with robotic arm.

We compared HyperArc to CyberKnife_G4, whereas Henzen et al[23] evaluated the more recent CyberKnife_M6 with different wall monitor-unit distributions than G4. In addition, v. M6 improves the machine positioning and trajectory compared to G4,[23,24] and its plan may also improve OAR sparing. Furthermore, v. M6 has a multimulleaf collimator that can provide enhanced concentration for large tumors. However, no report comparing CyberKnife G4 and M6 is available. In addition, the Multiplan (Accuray, Inc.) treatment planning system in this study was not the latest version available. Recently, a new treatment planning system, Precision (Accuray, Inc.), equipped with the VOLO™ optimizer was released for clinical practice and can reduce the planning and treatment delivery times. Therefore, the difference of beam-on time may be shortened using the more recent Precision system.

A low GI indicates a steeper dose decline. Ornelas-Couto et al[25] compared CyberKnife to VMAT for spine tumors in terms of GI and CI, and no considerable differences were found among these systems. In the present study, the CI and GI for HyperArc were significantly better than those for CyberKnife. Similarly, Ohira et al[9] found that HyperArc delivers better conformity than standard and noncoplanar VMAT. These results suggest that HyperArc has better conformity than CyberKnife.

Regarding the relations among volume doses V_3, V_6, and V_{12} with PTV (Figure 4), the line slopes of the regression for CyberKnife_G4 were higher than those for HyperArc, because the latter achieves lower GI for large targets. In fact, the slopes for CyberKnife_G4 were about two times those for HyperArc. These results suggest that HyperArc can accurately concentrate the dose to a target particularly in large tumors. Furthermore, the beam-on time of HyperArc is independent of the PTV, whereas that of CyberKnife_G4 increased with the tumor size. Hence, HyperArc contributes more than CyberKnife_G4 to treat large targets than small ones. For the volume dose in brain minus PTV, the median values for CyberKnife_G4 and HyperArc were almost the same because the analyzed cases were biased towards small targets, where the irradiated volume is usually small given the volume. Nevertheless, increasing OAR sparing for large targets should be the goal of more efficient treatments.

CONCLUSIONS

In this study, we investigated the dosimetric performance for HyperArc and compared it to CyberKnife_G4 in single and multiple brain metastases. In cases of single brain metastasis, the plan quality of HyperArc reached the level of the CyberKnife_G4 plans used in clinical practice, but the dose level for HyperArc depended on the defined margin. In cases of multiple brain metastases, decreasing the low dose for normal brain tissue depends on the distance among targets. Moreover, the delivery time for HyperArc does not depend on the PTV. Overall, we consider that HyperArc is best suited for larger targets in single brain metastasis and for smaller inter tumor distances in multiple brain metastases.

ACKNOWLEDGMENT

The authors (YU, SO, MM, and TT) would like to acknowledge Varian Medical Systems for providing the Eclipse system prototype, technical and financial support.

CONFLICTS OF INTEREST

The authors (YU, SO, MM, and TT) are currently collaborating with Varian Medical Systems, which provided financial support.

REFERENCES

1. Cairncross JG, Kim JH, Posner JB. Radiation therapy for brain metastases. *Ann Neurol* 1980; **7**: 529–41. doi: https://doi.org/10.1002/ana.410070606
2. Aoyama H, Tago M, Shirato H, Stereotactic radiosurgery with or without whole-brain radiotherapy for brain metastases: secondary analysis of the JROSG 99-1 randomized clinical trial. *JAMA Oncol* 2015; **1**: 457–64. doi: https://doi.org/10.1001/jamaoncol.2015.1145
3. Gevaert T, Levivier M, Lacornerie T, Verellen D, Engels B, Reynaert N, et al. Dosimetric comparison of different treatment modalities for stereotactic radiosurgery of arteriovenous malformations and acoustic neuromas. *Radiother Oncol* 2013; **106**: 192–7. doi: https://doi.org/10.1016/j.radonc.2012.07.002
4. Kuo JS, Yu C, Petrovich Z, Apuzzo MLJ. The CyberKnife stereotactic radiosurgery system: description, installation, and an initial evaluation of use and functionality. *Neurosurgery* 2003; **53**: 1235–9. doi: https://doi.org/10.1227/01.NEU.0000089485.47590.05
5. Echner GG, Kilby W, Lee M, Earnst E, Sayeh S, Schlaefer A, et al. The design, physical properties and clinical utility of an iris collimator for robotic radiosurgery. *Phys Med Biol* 2009; **54**: 5359–80. doi: https://doi.org/10.1088/0031-9155/54/18/001
6. Lai Y, Chen S, Xu C, Shi L, Fu L, Ha H. Dosimetric superiority of flattening filter free beams for single fraction stereotactic radiosurgery in single brain metastasis. *Oncotarget* 2016;: 1–8.
7. Lang S, Shrestha B, Graydon S, Cavelaars F, Linsenmeier C, Hrbacek J, et al. Clinical application of flattening filter free beams for extracranial stereotactic radiotherapy. *Radiother Oncol* 2013; **106**: 255–9. doi: https://doi.org/10.1016/j.radonc.2012.12.012
8. Stieler F, Fleckenstein J, Simeonova A, Wenz F, Lohr F. Intensity modulated radiosurgery of brain metastases with flattening filter-free beams. *Radiother Oncol* 2013; **109**: 448–51. doi: https://doi.org/10.1016/j.radonc.2013.10.017
9. Ohira S, Ueda Y, Akino Y, Hashimoto M, Masaoka A, Hirata T, et al. HyperArc VMAT planning for single and multiple brain metastases stereotactic radiosurgery: a new treatment planning approach. *Radiat Oncol* 2018; **13**: 1–9. doi: https://doi.org/10.1186/s13014-017-0948-z
10. Ruggieri R, Naccarato S, Mazzola R, Ricchetti F, Corradini S, Fiorentino A, et al. Linac-based VMAT radiosurgery for multiple brain lesions: comparison between a conventional multi-isocenter approach and a new dedicated mono-isocenter technique. *Radiat Oncol* 2018; **13**: 1–9. doi: https://doi.org/10.1186/s13014-018-0985-2
11. Slosarek K, Bekman B, Wendykier J, Grządziel A, Fogliata A, Cozzi L. In silico assessment of the dosimetric quality of a novel, automated radiation treatment planning strategy for linac-based radiosurgery of multiple brain metastases and a comparison with robotic methods. *Radiat Oncol* 2018; **13**: 41. doi: https://doi.org/10.1186/s13014-018-0997-y
12. Timmerman RD. An overview of hypofractionation and Introduction to this issue of seminars in radiation oncology. *Semin Radiat Oncol* 2008; **18**: 215–22. doi: https://doi.org/10.1016/j.semradonc.2008.04.001
13. Shaw E, Kline R, Gillin M, Souhami L, Hirschfeld A, Dinapoli R, et al. Radiation therapy Oncology group: radiosurgery quality assurance guidelines. *Int J Radiat Oncol Biol Phys* 1993; **27**: 1231–9. doi: https://doi.org/10.1016/0360-3016(93)90548-A
14. Paddick I, Lippitz B. A simple dose gradient measurement tool to complement the conformity index. *J Neurosurg* 2006; **105**(Supplement): 194–201. doi: https://doi.org/10.3171/sup.2006.105.7.194
15. Maranzano E, Trippa F, Casale M, Costantini S, Anselmo P, Carletti S, et al. Reirradiation of brain metastases with radiosurgery. *Radiother Oncol* 2012; **102**: 192–7. doi: https://doi.org/10.1016/j.radonc.2011.07.018
16. Combs SE, Schulz-Ertner D, Thilmann C, Edler L, Debus J. Treatment of cerebral metastases from breast cancer with stereotactic radiosurgery. *Strahlenther Onkol* 2004; **180**: 590–6. doi: https://doi.org/10.1007/s00066-004-1299-x
17. Barnett GH, Linskey ME, Adler JR, Cozzens JW, Friedman WA, Heilbrun MP, et al. Stereotactic radiosurgery--an organized neurosurgery-sanctioned definition. *J Neurosurg* 2007; **106**: 1–5. doi: https://doi.org/10.3171/jns.2007.106.1.1
18. Kelly PJ, Lin NU, Claus EB, Quant EC, Weiss SE, Alexander BM, et al. Salvage stereotactic radiosurgery for breast cancer brain metastases: outcomes and prognostic factors. *Cancer* 2012; **118**: 2014–20. doi: https://doi.org/10.1002/cncr.26343
19. Murphy MJ. Intrafraction geometric uncertainties in frameless image-guided radiosurgery. *Int J Radiat Oncol Biol Phys* 2009; **73**: 1364–8. doi: https://doi.org/10.1016/j.ijrobp.2008.06.1921
20. Murphy MJ, Chang SD, Gibbs IC, Le Q-T, Hai J, Kim D, et al. Patterns of patient movement during frameless image-guided radiosurgery. *Int J Radiat Oncol Biol Phys* 2003; **55**: 1400–8. doi: https://doi.org/10.1016/S0360-3016(02)04597-2
21. Hoogeman MS, Nuyttens JJ, Levendag PC, Heijmen BJM. Time dependence of intrafraction patient motion assessed by repeat stereoscopic imaging. *Int J Radiat Oncol Biol Phys* 2008; **70**: 609–18. doi: https://doi.org/10.1016/j.ijrobp.2007.08.066
22. Fu D, Kuduvalli G, Mitrovic V, Main W, Thomson L. Auto-mated skull tracking for the CyberKnife image-guided radiosurgery sys-tem. *Proc. SPIE* 2005; **5744**: 366–77.
23. Henzen D, Schmidhalter D, Zanella CC, Volken W, Mackeprang P-H, Malthaner M, et al. Evaluation of clinically applied treatment beams with respect to bunker shielding parameters for a Cyberknife M6. *J Appl Clin Med Phys* 2018; **19**: 243–9. doi: https://doi.org/10.1002/acm2.12215
24. Yang J, Feng J. Radiation shielding evaluation based on five years of data from a busy CyberKnife center. *Journal of Applied Clinical Medical Physics* 2014; **15**: 313–22. doi: https://doi.org/10.1120/jacmp.v15i6.4575
25. De Ornelas-Couto M, Bossart E, Ly B, Monterroso MI, Mihaylov I. Radiation therapy for stereotactic body radiation therapy in spine tumors: linac or robotic? *Biomed Phys Eng Express* 2016; **2**: 015012. doi: https://doi.org/10.1088/2057-1976/2/1/015012